Comparative Evaluation of Harmonic Compensation Capability of Active Power Filter with Conventional and Bacterial Foraging Based Control

S. S. Patnaik* and Prof. A. K. Panda

Department of Electrical Engineering, National Institute of Technology, Rourkela, India
E-mail: sspatnaik.ee@gmail.com, akpanda.ee@gmail.com

***Abstract*- Optimizing the performance of power system networks using conventional methods is quite difficult because of the complex nature of systems that are highly non-linear and non-stationary. In this paper, it is proposed to implement Bacterial foraging (BF) optimization to the conventional shunt active power filter (APF). A comparative analysis of the APF performance is carried out for BF based and conventional approach under unbalanced supply voltage. The instantaneous active and reactive current components (i_d-i_q) method of reference compensation current generation; having greater sensitivity to harmonics and unbalances has been utilized here. Extensive MATLAB simulations are carried out and results demonstrate that the APF with proposed implementation of BF algorithm outperforms the conventional APF in terms of both convergence rate and current harmonic compensation.**

I. INTRODUCTION

Intensification of harmonic pollution in the power system at an alarming rate has brought down the efficiency and power factor, with increase in the risk of electromagnetic interference with the neighboring communication lines. This is principally due to the proliferation of typical non-linear loads such as arc furnaces, fluorescent lights, power electronic converters, microprocessors, motor drives, electronic loads, saturated transformers, various domestic appliances, etc. that draw significant amount of harmonic current from the utility.

The shunt APF is intended to be used not merely for compensation of current harmonics but also for unbalance in the source current generated due to non-linear loads. It injects current harmonics of equal magnitude and opposite phase at the point of common coupling (PCC) between the source and the load [1]. For proper functioning of APF it is crucial to design an appropriate control scheme. In conventional instantaneous active and reactive power (*p*-*q*) method, the reactive power and oscillating component of active power are used for the generation of reference compensation currents [2], [3]. The multiplication of instantaneous load currents and voltages while calculating the instantaneous powers caused amplification of harmonic content leading to imprecise harmonic compensation. Later, the instantaneous active and reactive current component (i_d-i_q) method is proposed to replace the *p*-*q* method, bringing down the total harmonic distortion (THD) in supply current below 5% so as to satisfy the IEEE-519 standard even when the supply voltage is not ideal [4], [5]. In this paper, the performance of active filter with conventional control is improved by means of BF algorithm, since the conventional approach becomes complex to implement as the power system represents a highly non-linear and non-stationary system. Moreover, the conventional control yields inadequate result at every operating point except the one at which it is designed to be operated [6], [7].

The BF optimization technique is briefly explained in Section II. Section III describes the system configuration of shunt connected APF, Section IV the simulation results, and the conclusion is summarized in Section V.

II. BACTERIAL FORAGING OPTIMIZATION

This optimal foraging theory initially proposed by Passino [8] and further established by Mishra [9], formulates the foraging behavior exhibited by *E.coli* bacteria inside human intestine, in which they search for and obtain nutrients in a way that maximizes their energy intake (E) per unit time (T), as non-gradient optimization problem. BF mimics four principal mechanisms observed in bacteria viz. chemotaxis, swarming, reproduction and elimination-dispersal.

A. Chemotaxis

The movement of *E.coli* bacteria in the human intestine in search of nutrient-rich location away from noxious environment is accomplished with the help of the locomotory organelles known as flagella by chemotactic movement in either of the ways i.e. swimming (in the same direction as the previous step) or tumbling (in a absolutely different direction from the previous one). Suppose $\theta^i(j,k,l)$ represents the i^{th} bacterium at j^{th} chemotactic, k^{th} reproductive and l^{th} elimination-dispersal step. Then chemotacic movement of the bacterium may be mathematically represented by the following equation.

$$\theta^i(j+1,k,l) = \theta^i(j,k,l) + C(i)\frac{\Delta(i)}{\sqrt{\Delta^T(i)\cdot\Delta(i)}} \quad (1)$$

In the expression, $C(i)$ is the size of the unit step taken in the random direction and $\Delta(i)$ indicates a vector in the arbitrary direction whose elements lie in [-1, 1].

B. Swarming

This group behavior is seen in several motile species of bacteria, where the cells when stimulated by a high level of

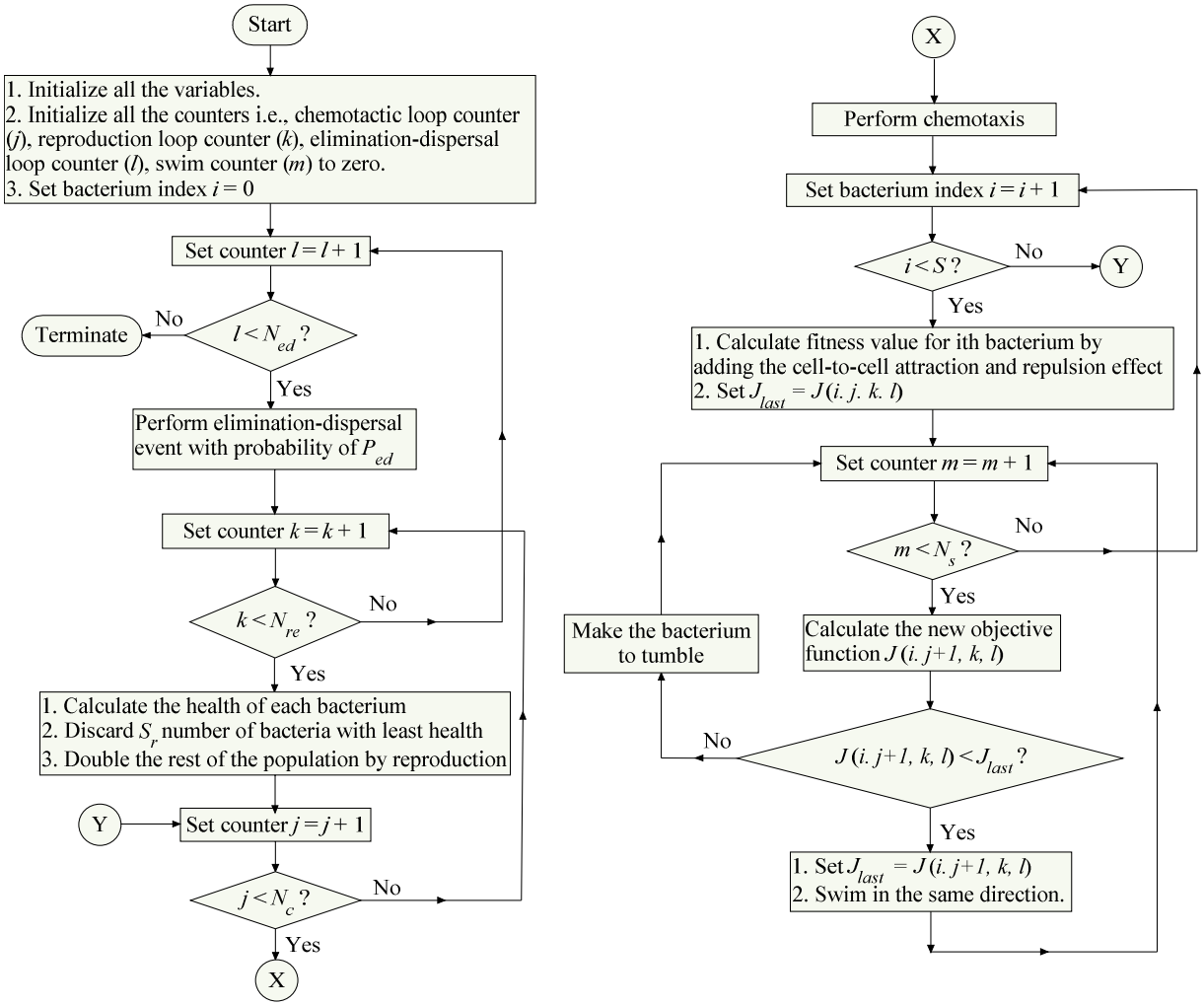

Fig.1. Flowchart of BF algorithm

succinate, release an attractant *aspertate*. This helps them propagate collectively as concentric patterns of swarms with high bacterial density while moving up in the nutrient gradient. The cell-to-cell signaling in bacterial swarm via attractant and repellant may be modeled as per (2) where $J_{cc}(\theta(i, j, k, l))$ specifies the objective function value to be added to actual objective function that needs to be optimized, to present a time varying objective function.

$$J_{cc}(\theta(i,j,k,l)) = \sum_{i=1}^{S} J_{cc}(\theta, \theta^i(j,k,l))$$
$$= \sum_{i=1}^{S}\left[-d_{attractant}\exp(-w_{attractant}\sum_{m=1}^{p}(\theta_m - \theta_m{}^i)^2)\right]$$
$$+ \sum_{i=1}^{S}\left[h_{repellant}\exp(-w_{repellant}\sum_{m=1}^{p}(\theta_m - \theta_m{}^i)^2)\right] \quad (2)$$

Here S indicates the total number of bacteria in the population, p is the number of variables to be optimized, $\theta = [\theta_1, \theta_2, \ldots, \theta_p]^T$ is a point in the p-dimensional search domain. The coefficients $d_{attractant}$, $w_{attractant}$, $h_{repellant}$ and $w_{repellant}$ are the measure of quantity and diffusion rate of the attractant signal and the repellant effect magnitude respectively.

C. Reproduction

The fitness value for i^{th} bacterium after travelling N_c chemotactic steps can be evaluated using (3).

$$J^i_{health} = \sum_{j=1}^{N_c+1} J^i(j,k,l) \quad (3)$$

Here $J^i{}_{health}$ represents the health of i^{th} bacterium. The least healthy bacteria constituting half of the bacterial population are eventually eliminated while each of the healthier bacteria asexually split into two, which are then placed in the same location. Hence, ultimately the population remains constant.

D. Elimination and dispersal

The BF algorithm makes some bacteria to get eliminated and dispersed with probability P_{ed} after N_{re} number of reproductive events to ensure that the bacteria do not get trapped into a local optimum instead of the global optima. The BF algorithm flowchart is presented in Fig.1.

III. APF System Configuration

The system configuration of a 3-phase 3-wire shunt APF is depicted in Fig.2. The performance of filter is studied under

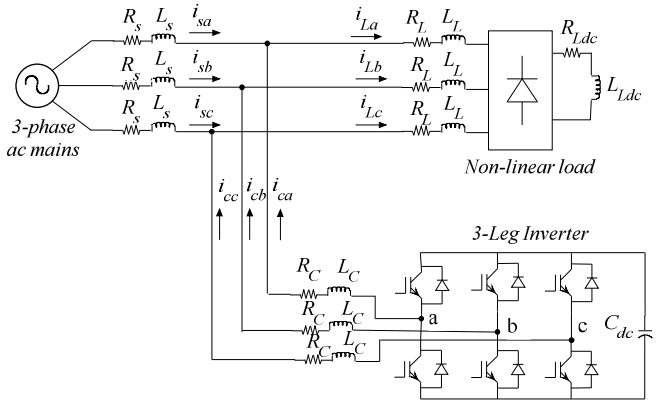

Fig.2. Shunt active filter configuration along with non-linear load

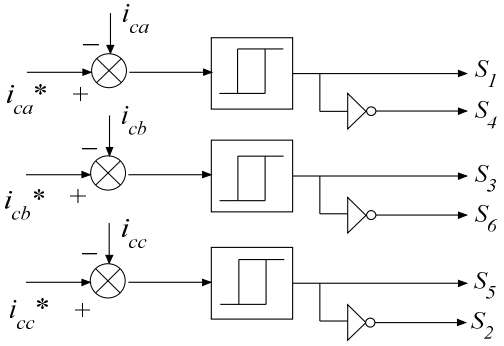

Fig.4. Generation of switching signals with Hysteresis comparator

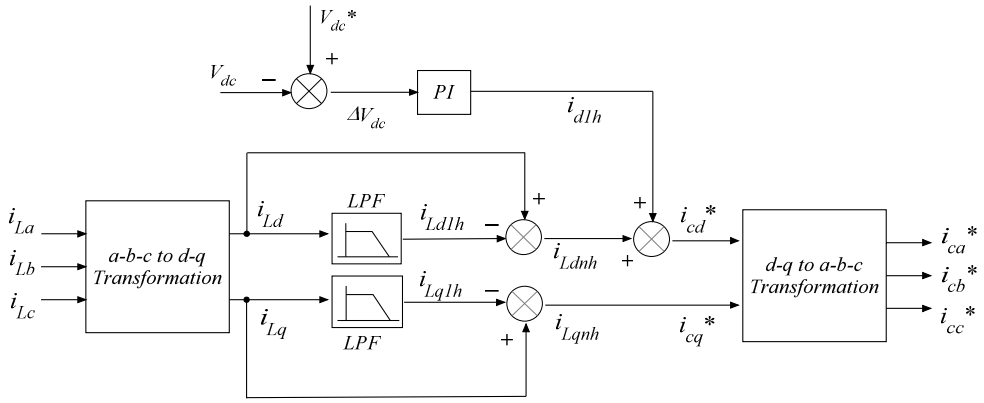

Fig.3. Reference compensation current extraction scheme

unbalanced supply condition. Here the non-linear load consisting of diode rectifier is the current-source type harmonic source. The APF is comprised of a VSI with hysteresis PWM current control. Controller for the APF is designed using i_d-i_q control scheme. Inputs to the controller are the three-phase load currents and the DC-link capacitor voltage of the inverter. The gains of the PI controller used for DC-link voltage regulation is optimized using conventional and BF techniques. Output of the controller is reference compensation current template. The filter currents and the reference currents are compared in a hysteresis comparator giving away required current pulses for switching actions to be carried out in the switching devices of the VSI. Finally the filter generated compensation current is injected into the power system at PCC to assure that sinusoidal and compensated current is drawn from the utility.

A. DC-link voltage controller

While operating under steady state condition of the shunt APF, the VSI should neither absorb nor deliver active power. So the main concern lies in getting an optimally tuned PI controller which satisfies the conditions of dynamics and stability both by making the dynamics of inverter DC- link voltage (V_{dc}) sufficiently low. In various conventional PI controller tuning methods such as Ziegler-Nichols method, the recommended settings are empirical in nature and require extensive experimentation. Hence there is always scope for improving the PI controller tuning that yields suitable values of proportional gain (K_p) and integral gain (K_i) for which it gives better settling time within tolerable limits of maximum overshoot. This purpose can be accomplished by implementing BF to minimize the deviation of V_{dc} from its reference V_{dc}* value. Maximum overshoot (ΔV_{dcmax}), rise time (t_r) and steady-state error (E_{ss}) are the constraints that imply the optimality of PI controller. The objective here is to reduce the DC-link voltage deviation ($\Delta V_{dc} = V_{dc}^* - V_{dc}$).

The performance criteria chosen in this paper is Integral Square Error (ISE) and the objective function to be optimized (J) is estimated using (4), where α and β symbolize weighing factors, t_0 is the starting time and t_s is the settling time of transient. The significance of weighing factors is that; α is used to overcome the steady-state voltage error E_{ss} and β decides the values of ΔV_{dcmax} and t_s. Large value of β results in less overshoot whereas, smaller value of β results in reduced settling time.

$$J = \int_0^t \left(\Delta V_{dc}\right)^2 dt = \beta \cdot \Delta V_{dc\max} + (1-\beta)(t_s - t_0) + \alpha \cdot \left|E_{ss}\right| \quad (4)$$

B. Reference compensation current extraction

The PI controller output signal i_{d1h} represents the total active current required to maintain the DC-link voltage at a constant level and to compensate the losses in the APF due to the presence of inductances and semiconductor switches. The three-phase load currents (i_{La}, i_{Lb}, i_{Lc}) are tracked by the use of current sensors, upon which Park's transformation is carried

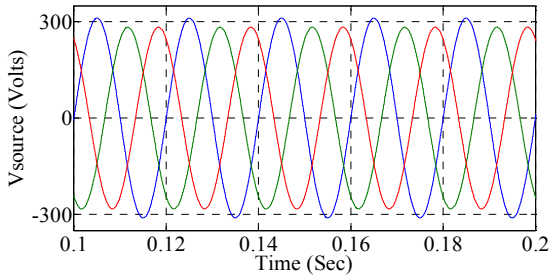

Fig.5. Unbalanced supply voltage waveform

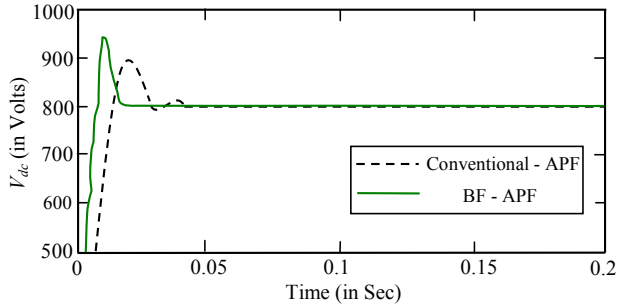

Fig.6. Convergence characteristics of V_{dc}

out in order to get the corresponding *d-q* axes current components i_{Ld} and i_{Lq} with the help of (5). According to i_d-i_q control strategy, the load should only draw the average value of direct-axis component of load current from the supply. Here i_{Ld1h} and i_{Lq1h} indicate the fundamental frequency component of the currents i_{Ld} and i_{Lq} respectively.

$$\begin{bmatrix} i_{Ld} \\ i_{Lq} \end{bmatrix} = \begin{bmatrix} i_{Ld1h} + i_{Ldnh} \\ i_{Lq1h} + i_{Lqnh} \end{bmatrix} = \begin{bmatrix} \sin wt & \cos wt \\ -\cos wt & -\sin wt \end{bmatrix} \begin{bmatrix} 1 & -\frac{1}{2} & -\frac{1}{2} \\ 0 & \frac{\sqrt{3}}{2} & -\frac{\sqrt{3}}{2} \end{bmatrix} \begin{bmatrix} i_{La} \\ i_{Lb} \\ i_{Lc} \end{bmatrix} \quad (5)$$

The oscillating components of the currents i_{Ld} and i_{Lq} i.e. i_{Ldnh} and i_{Lqnh} respectively are filtered out by using Butterworth low-pass filter with cut-off frequency $f_c = f/2$ (f = fundamental supply frequency). The currents i_{Ldnh} and i_{Lqnh} along with i_{d1h} are utilized to generate the desired reference compensation filter currents i_{cd}* and i_{cq}* in *d-q* coordinates, followed by inverse Park transformation giving away the three-phase compensating currents i_{ca}*, i_{cb}* and i_{cc}* in *a-b-c* reference frame as described in (6). The zero-sequence current i_{c0}* is brought into play in order to make the transformation matrix a square one.

$$\begin{bmatrix} i_{ca}^* \\ i_{cb}^* \\ i_{cc}^* \end{bmatrix} = \begin{bmatrix} \sin wt & \cos wt & 1 \\ \sin(wt - 2\pi/3) & \cos(wt - 2\pi/3) & 1 \\ \sin(wt + 2\pi/3) & \cos(wt + 2\pi/3) & 1 \end{bmatrix} \begin{bmatrix} i_{cd}^* \\ i_{cq}^* \\ i_{c0}^* \end{bmatrix} \quad (6)$$

In Fig.3 the scheme of reference current generation for shunt APF using i_d-i_q method has been illustrated. This scheme does not require a Phase locked loop (PLL) as only current quantities are involved; hence synchronization between phase currents and voltages is not needed.

The reference signals thus obtained are compared with the actual compensation filter currents in a hysteresis comparator as shown in Fig.4, where the actual current is forced to follow

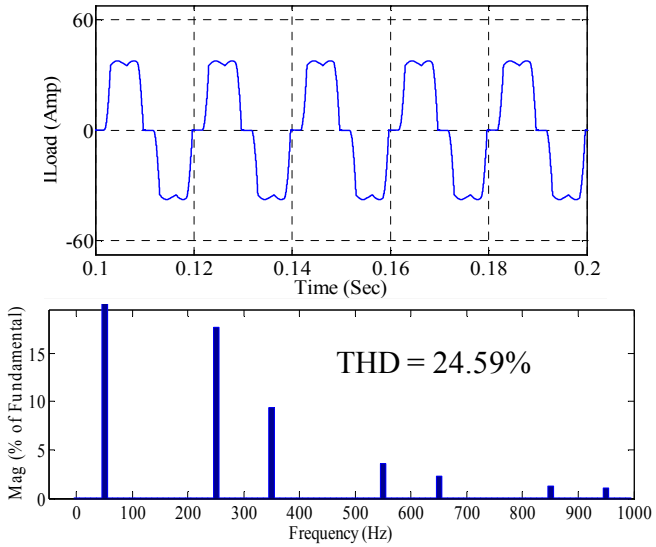

Fig.7. Load current waveform and its THD

the reference. Hysteresis band current controller is preferred to be used on account of its easy implementation and quick prevail over fast current transitions and instantaneous compensation by the APF. This consequently provides the switching signals S_1, S_3 and S_5 to trigger the IGBTs in upper arm of VSI, whereas the respective inverted signals S_4, S_6 and S_2 are used to trigger the switches corresponding to lower arm of the inverter. Ultimately, it provides necessary compensation for harmonics in the source current and reactive power unbalance in the system.

IV. Simulation Results

The shunt APF performance is evaluated by taking into consideration its (a) harmonic compensation capability and (b) dynamic performance under unbalanced supply voltage as shown in Fig.5. The APF performance is analyzed with the error between DC-link voltage and its reference value being regulated by the conventionally tuned PI controller followed by optimally tuned PI controller. The simulation is performed taking the parameter values as listed in Table I. It can be seen from V_{dc} convergence characteristics as depicted in Fig.6, the BF based PI controller offers faster convergence to reach the optimal solution and hence quicker prevail over harmonic disturbances compared to the conventional PI controller.

TABLE I
SYSTEM PARAMETERS USED FOR SIMULATION

System parameter	Symbol	Value
Supply frequency	f	50 Hz
Source impedance	R_s, L_s	0.1 Ω, 0.01 mH
AC-side filter impedance	R_c, L_c	0.1 Ω, 1 mH
DC-side filter capacitance	C_{dc}	3000 µF
DC-link voltage reference	V_{dc}*	800 V
DC-side load parameters	R_{Ldc}, L_{Ldc}	20 Ω, 25 mH
AC-side load parameters	R_L, L_L	0.1 Ω, 3 mH

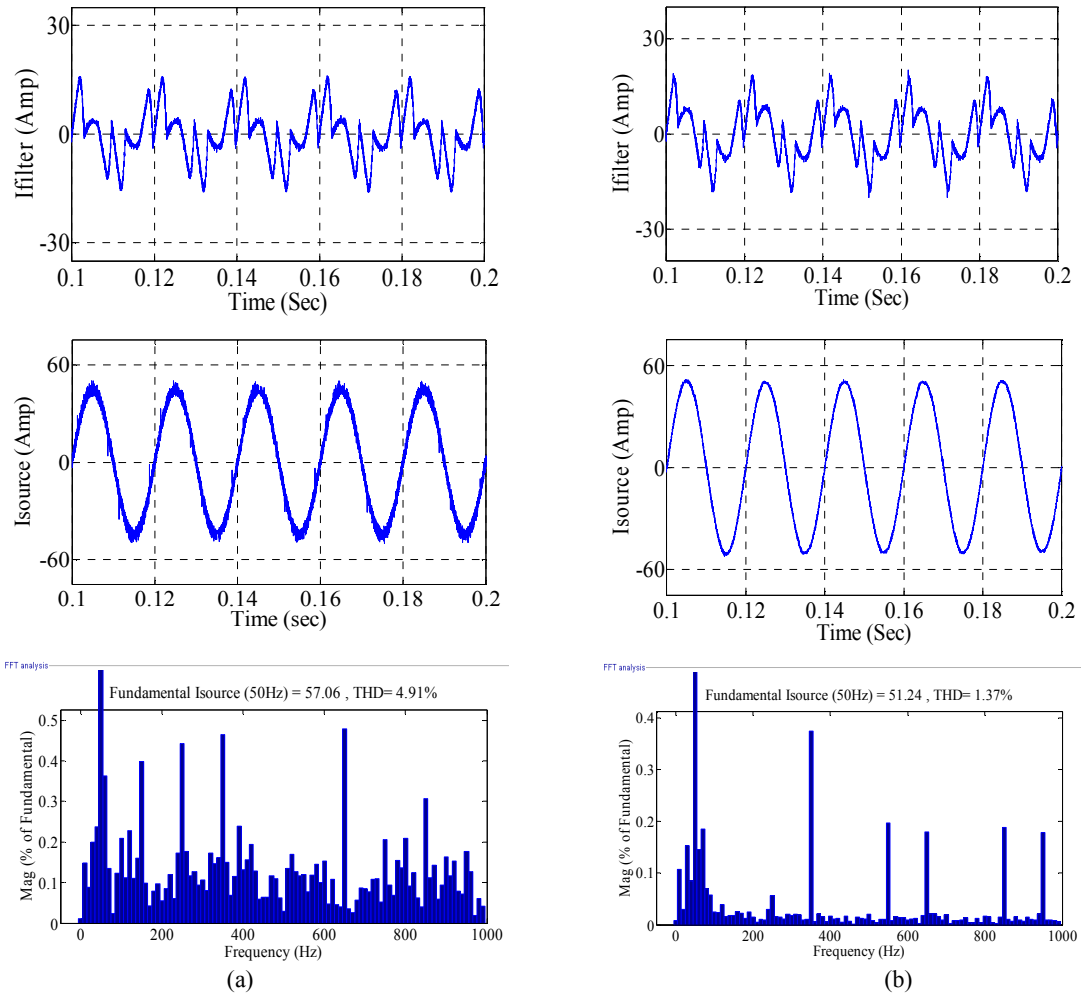

Fig.8. Simulation waveforms for compensation current, source current and its THD with (a) BF-PI and (b) Conventional-PI based APF

When the APF is not being operated, the load current (ILoad) is exactly reflected in source current i.e. the source current THD is 24.59% before compensation, which is depicted in Fig.7. The performance of shunt APF employing BF-PI has been compared with the conventional-PI based APF. The nature of compensation filter current (Ifilter), compensated source current (Isource) and its FFT analysis showing the THD have been displayed in Fig.8 for APFs employing conventional and BF based PI controllers. It was observed that source current THD is 4.91% for APF employing conventional-PI which is drastically lowered down to 1.37% by employing BF, which signifies excellent functionality of shunt APF with the proposed implementation of BF.

V. CONCLUSION

The simulation results demonstrate that the active filter employing BF yields superior harmonic compensation over conventionally controlled APF. To verify its robustness, the evaluation was carried out taking huge unbalance in supply voltage. It is revealed that, the proposed implementation of BF algorithm offers faster convergence, superior transient settling time within permissible values of maximum over shoot, thereby fulfilling the ultimate objective of lowering down the value of THD in source current.

REFERENCES

[1] B. Singh, K. Al-Haddad, A. Chandra, "A review of active filters for power quality improvement," *IEEE Trans. Ind. Electron.*, Vol. 46, No. 5, pp. 960-971 Oct. 1999.

[2] H. Akagi, E. H. Watanabe, M. Aredes, "Instantaneous power theory and applications to power conditioning," *IEEE Press/Wiley-Inter-science,* New Jersey, 2007.

[3] H. Akagi, Y. Kanazawa, A. Nabae, "Instantaneous reactive power compensators comprising switching devices without energy storage components," *IEEE Trans. Ind. Applications*, Vol. IA-20, No. 3, pp. 625–630, May/Jun. 1984.

[4] V. Soares, P. Verdelho, G. D. Marques, "An instantaneous active and reactive current component method for active filters," *IEEE Trans. Power Electron.*, Vol. 15, No. 4, pp. 660-669, Jul. 2000.

[5] M. Montero, E. R. Cadaval, F. B. Gonzalez, "Comparison of control strategies for shunt active power filters in three-phase four-wire systems," *IEEE Trans. Power Electron.*, Vol. 22, No. 1, pp. 229-236, Jan. 2007.

[6] S. H. Zak, "Systems and control," 1st ed., *Oxford University Press*, New York, 2003, pp. xv-574.

[7] C. A. Smith, A. B. Corripio, "Automatic processes control," 1st ed. México D.F., México, 1991, pp. 212-296.

[8] K. M. Passino, "Biomimicry of bacterial foraging for distributed optimization and control," *IEEE Control System Magazine*, pp. 52-67, Jun. 2002.

[9] S. Mishra, C. N. Bhende, "Bacteria foraging technique-based optimized active power filter for load compensation," *IEEE Trans. Power Delivery*, Vol. 22, No. 1, pp. 457-465, Jan. 2007.